International Immunopharmacology 70 (2019) 135–146

Contents lists available at ScienceDirect

International Immunopharmacology

journal homepage: www.elsevier.com/locate/intimp

MiR-128 mediates negative regulation in *Staphylococcus aureus* induced inflammation by targeting MyD88

Xiaofei Ma, Shuai Guo, Kangfeng Jiang, Xiaoyan Wang, Nannan Yin, Yaping Yang, Arshad Zahoor, Ganzhen Deng*

Department of Clinical Veterinary Medicine, College of Veterinary Medicine, Huazhong Agricultural University, Wuhan, China

ARTICLE INFO

Keywords:
ALI
S. aureus
miR-128
MyD88
NF-κB

ABSTRACT

Acute lung injury (ALI) is a common clinical syndrome of excessive uncontrolled inflammatory response in lung tissues with high mortality rates and limited therapeutic approaches. MicroRNAs (miRNAs) are a class of small non-coding RNAs which attach at 3′UTR of mRNA for further regulation of diverse proteins. MiRNAs are a current focus in regulating the inflammatory processes. The extent of pro-inflammatory gene activated against *Staphylococcus aureus* (*S. aureus*) is still unclear. Myeloid differentiation primary response 88 (MyD88) is involved in gram positive bacteria-induced lung inflammation by Toll-like receptors (TLRs). Then MyD88 activates NF-κB through IRAKs which are in charge of inflammation. Target prediction analyses revealed MyD88, a result of projections from multiple bio-websites, to be a putative target of miR-128. Here we probe the expression of the MyD88 and miRNA in mode of inflammation. We found up-regulated expression of MyD88 and down-regulation of miR-128 after *S. aureus* infection in mouse lung tissues and RAW264.7 cells via qPCR and western blotting (WB) analysis. Moreover, MyD88-miR-128 interaction was validated by luciferase assays. Then, we proved that miR-128 expression caused a reduction in IκBα and p65 phosphorylation and resulted in significant reduction in secretion of inflammatory cytokines, being consistent with the deletion of MyD88 in macrophages. It revealed that miR-128 specifically blocked the further development of inflammation through MyD88 down-regulation. Finally, we demonstrated a novel role of miR-128 that it mediates negative regulation in *S. aureus* induced inflammation by targeting MyD88.

1. Introduction

Acute lung injury (ALI) is a severe inflammatory syndrome caused by direct lung damage or injury, including via bacterial infection [1], with bilateral lung infiltration, high mortality, which leads to a substantial health burden all over the world [2,3]. It is mostly caused by sepsis, inhalation injury and pneumonia [4]. Clinically, sepsis, which is a severe infection of the bloodstream, is the most common cause of ALI [1] and occurs often by *S. aureus* infection. *S. aureus* is a wide range of commensal bacteria and pathogens.

During the pathogenesis of ALI, a large number of neutrophils which produced pro-inflammatory mediators that damaged lung epithelial cells were recruited [5]. Immune cells release cytokines and chemokines such as IL-Iβ, IL-6, TNF-α and MCP-1 in response to lung injury, eventually resulting in leading to an acute inflammatory response. Although many biomarkers and supportive treatments for ALI have emerged in recent years [6], much remains unknown. Therefore, more research is needed for the diagnosis and treatment of ALI.

In recent years, the unique regulation of miRNA in various biological processes has caught the attention. MiRNAs are a class of small, non-coding RNAs, about 19–25 nucleotides in length widely found in eukaryotes, which can negatively regulate target genes through the inhibition of mRNA transcription and translation, and are key elements of intracellular signaling [5,7]. The identity of miRNAs as a gene regulatory factor has been examined for disease diagnosis in multiple fields such as inflammation, diabetes, apoptosis, cancer, tumor and autoimmune diseases [8–14]. MiRNA exhibits characteristic expression signatures in various types of inflammation and can profoundly affect the behavior of inflammatory cells. Due to that miRNAs have differential expression in different cell types and tissues and in various biological processes, they may be useful for treatment methods [15,16].

An increasing number of miRNA-based therapies are currently under study. Sonkoly et al. are pioneers showing the involvement of miRNAs in inflammatory diseases [17]. Subsequently, a large quantity of inflammation-related miRNAs that can regulate inflammatory responses were discovered, such as miR-21, miR-124 and miR-125a-5p

* Corresponding author.
E-mail address: ganzhendeng@sohu.com (G. Deng).

https://doi.org/10.1016/j.intimp.2018.11.024
Received 11 July 2018; Received in revised form 14 November 2018; Accepted 15 November 2018
Available online 22 February 2019

[18–20]. Recently, studies to determine the genetic components of ALI pathogenesis have investigated the involvement of miRNAs in this process [21]. The microRNA-128 (miR-128) is a multifunctional regulator involved in cell apoptosis [22], cancer [23], tumor [24] and inflammation [25–28]. In particular, it is noteworthy that recent studies have found that the expression of miR-128 is abnormal in the gingival tissue of patients with periodontitis [29], and further indicates that the enhanced expression of miR-128 can reduce the secretion of TNF-α and inhibit p38 phosphorylation, which further relieve the development of inflammatory macrophages. Studies have also found that miR-128 plays a key role in rheumatoid arthritis and inflammation of rat kidney cells in vitro [5,30].

Here, miR-128 is one of the miRNAs concerning with inflammatory responses. It has been reported that miR-128 could negatively regulate lipopolysaccharide-induced lipid accumulation and inflammatory responses in macrophages by the TLR4-NF-κB pathway [22]. In this study, we characterized miR-128 expression in ALI mouse lung tissues and in RAW264.7 macrophages stimulated with *S. aureus* and investigated the effects of miR-128 on inflammation in RAW264.7 macrophages and ALI. The results showed that miR-128 targeted the 3′UTR of MyD88 mRNA and modulated its expression, which suggests that miR-128 might suppress *S. aureus*-induced inflammatory response by targeting MyD88.

2. Materials and methods

2.1. Chemical reagents and antibodies

Mouse monoclonal antibodies against MyD88, IKK (IKKα/β), p-IKKα/β, IκBα, p-IκBα, p65, p-p65 and β-actin were obtained from Cell Signalling Technology (Beverly, MA, USA). The horseradish peroxidase (HRP) goat anti-rabbit and goat anti-mouse antibodies were also provided by Cell Signaling Technology (Beverly, MA, USA). Fetal bovine serum (FBS) was purchased from Sigma Inc. (St. Louis, MO, USA). All other chemical reagents were reagent grade.

2.2. Microbial strains

Staphylococcus aureus strain (ATCC 25923) was obtained from the American Type Culture Collection (ATCC, MD, USA) and cultured in Luria-Bertani (LB) broth (Oxoid, Hampshire, UK) at 37 °C and 200 rounds per minute. Bacterial stocks were kept at −80 °C in LB medium supplemented with 20% (vol/vol) of glycerol. Overnight cultures of *S. aureus* were re-inoculated into fresh LB and grown to log phase. The bacteria were then harvested by centrifugation, washed and resuspended in normal saline solution at the appropriate concentration for the final inoculum size. The inoculum size, in colony forming units (CFU), was confirmed by serial dilution and the plate count method.

2.3. Cell culture

The cells used in the study were RAW264.7 macrophages and purchased from the American Type Culture Collection (ATCC TIB-71™). To ensure that the cells are normal small pieces of round or elliptical cells, RAW264.7 macrophages was cultured in Dulbecco's modified Eagle's medium (DMEM, High Glucose) containing 10% FBS, 100 U/ml penicillin and 100 μg/ml streptomycin at 37 °C with 5% CO_2. The old medium was replaced by DMEM before the cells were stimulated with *S. aureus*.

RAW264.7 macrophages were seeded in 96-well cell culture plates at a density of 4.5×10^4 cells/well by a cell counting plate. The corresponding amount of *S. aureus* (4.5×10^5 CFU) was administered per well according to the infection index (MOI = *S. aureus*/cells = 10). The cells were stimulated with *S. aureus* (MOI = 10) for 0 h, 0.5 h, 1 h, 1.5 h, 2 h, 6 h, 12 h and 24 h. The 0 h time-point represents untreated cells served as the controls for our assays. *S. aureus* used to stimulate cells was resuspended with DMEM instead of PBS.

2.4. Animals and the ALI model

Healthy male BALB/c mice aged 6–8 weeks and weighing 25–30 g purchased from the Animal Experiment Center of Huazhong Agricultural University (Wuhan, China) were allowed to acclimate for 2 days before experimentation. All animals were maintained in a pathogen-free conditioned room at 24 ± 1 °C with 40%–80% humidity under a 12 h light/12 h dark cycle. Food and water were supplied libitum. All experimental procedures were conducted according to guidelines provided by the Laboratory Animal Research Center of Hubei province, and approved by the Ethical Committee on Animal Research at Huazhong Agricultural University (HZAUMO-2015-12).

In this study, we randomly divided the mice into two groups as follows: 1) The mouse model of *S. aureus*-induced lung tissues (*S. aureus*): The mice were stimulated with intratracheal instillation of *S. aureus* (1.6×10^8 CFU). 2) Control groups (Control): The mice were treated with nothing. In ALI model, we used a suspension of *S. aureus*, which was resuscitated as described in Section 2.2. *S. aureus* resuspended in 1000 μl PBS (1×10^7 CFU per 10 μl) were inoculated with 80 μl suspension per lung via the intranasal route for inducing infection in the lung tissues. From both sides of the nare, the nasal drops of bacterial slurry of 80 μl were injected, and mice were held upright for 1 min and then continued to keep the normal feeding for 24 h. All mice were euthanized 24 h after *S. aureus* exposure in all groups and we immediately sampled for subsequent experiments.

2.5. Lung histological assay

For histopathological examination, the lungs of mice were fixed in 4% paraformaldehyde for 24 h. Lung tissues were dehydrated with graded alcohol (100%, 95% and 90%), embedded in paraffin. Sections of 4 μm thicknesses were cut using a microtome and stained with hematoxylin and eosin (H&E). Subsequently, sections were assessed with a microscope (Olympus Shinjuku-ku, Tokyo, Japan).

2.6. Wet to dry weight (W/D) ratio of the lung and MPO assays

The mice were euthanized, and the wet-dry weight ratios were quantified to assess for vascular leak using the left lung. The wet weight was measured immediately, and then the lungs were dried at 80 °C for 48 h in a constant temperature oven and weighted again to determine the dry weight. The infiltration of neutrophils in the lung tissues was determined by measuring the activity of myeloperoxidase (MPO) using a MPO test kit (Nanjing, Jiangsu, China).

2.7. CCK-8 assay

In order to detect whether the cell viability is affected by treatment with inactivated *S. aureus*, macrophage viability was determined using a Cell Counting Kit-8 (CCK-8) assay kit (Beyotime, Shanghai, China). *S. aureus* was inactivated with 0.2% formaldehyde for 24 to 48 h at 37 °C to maintain the intact morphology of *S. aureus* and prevent bacterial growth without cytotoxicity. The cells were seeded into a 96-well plate at a density of 4.5×10^4 cells per well and stimulated with *S. aureus* (MOI = 10) at 0 h, 6 h, 12 h and 24 h later. The old medium in the wells was replaced with fresh medium, then CCK-8 reagent was added. The cells were continued for 4 h, after the time required for culture, the optical density (OD) value was measured at 450 nm with a microplate reader (Thermo Scientifc Multiskan MK3, USA).

2.8. Immunofluorescence assay

The RAW264.7 cells stimulated with *S. aureus* (MOI = 10) for 12 h were rinsed three times with PBS and then fixed with 4%

paraformaldehyde for 20 min. Slides were incubated with 0.5% Triton X-100 for 20 min, and then normal goat serum was added to the slides for 30 min at room temperature. Subsequently, the slides were incubated with p-p65 or MyD88 antibody (Beverly, MA, USA) overnight at 4 °C. The slides were incubated with fluorescent secondary antibody for 1 h in the wet box and then counterstained with DAPI for 5 min in the dark, and finally blocked with the anti-fluorescent quencher. The images were observed under a Leica TCS SP8 AOBS confocal laser-scanning microscope.

2.9. Computational predication of the miRNA targets

The possible target genes for miR-128 in mice were predicted with four algorithms from microRNA (http://34.236.212.39/microrna/getMirnaForm.do), TargetScan (http://genes.mit.edu/targetscan/), miRBase (http://www.mirbase.org/) and miRWalk (http://www.umm.uni-heidelberg.de/apps/zmf/mirwalk/index.html).

2.10. Transfection with miR-128 mimic and inhibitor

A miRNA-128 mimic (double-stranded RNA oligonucleotides), an inhibitor (single-stranded RNA oligonucleotides) for miR-128, negative control duplexes of the miRNA mimic (negative control) and an inhibitor were synthesized by GenePharma (Shanghai, China), and their sequences were shown in Table 1. After the cell density reached to 60–70% in a six well plate, RAW264.7 cells were transfected with the miR-128 mimic, the miR-128 inhibitor or their negative control duplexes using Lipofectamin™2000 (Invitrogen, Carlsbad, California, USA) according to the manufacture's instructions. After 6 h of transfection, the old medium was discarded and the cells were cultured in fresh DMEM containing 100 U/ml penicillin and 100 μg/ml streptomycin for 48 h. The samples were then collected for subsequent assay.

2.11. ELISA assay

One hundred milligrams of lung tissues were cut with an ophthalmic scissors on ice and then grinded into a powder. After adding RIPA (1 ml) to lyse the lung tissues and cells, the supernatants were collected by centrifugation at 12,000 rpm for 10 min at 4 °C from the lung tissues and cell culture. The collected supernatants were used to quantify IL-1β, IL-6 and TNF-α protein expression levels two times with ELISA kit (Bio-Swamp) according to the manufacture's protocols. OD of each well was determined at 450 nm using a microplate reader (Thermo Scientifc Multiskan MK3, USA) and the concentration of IL-1β, IL-6 and TNF-α was calculated by a linear standard curve.

Table 1
Primers for miR-128 and MyD88 siRNA.

Name	Primer sequence (5′–3′)
miR-128	Specific stem-loop primer: GTCGTATCCAGTGCAGGGTCCGAGG TATTCGCACTGGATACGACCCCCTA F: CTGTTAATGCTAATCGTGATAG R: GCAGGGTCCGAGGT
miR-128 mimic	F: UCACAGUGAACCGGUCUCUUU R: AGAGACCGGUUCACUGUGAUU
miR-128 mimic NC	F: UUCUCCGAACGUGUCACGUTT R: ACGUGACACGUUCGGAGAATT
miR-128 inhibitor	F: AAAGAGACCGGUUCACUGUGA
miR-128 inhibitor NC	F: CAGUACUUUUGUGUAGUACAA
MyD88 siRNA	F: UUUAUCUCCAGGUAAGUGCAG R: GCACUUACCUGGAGAUAAAGA
siRNA NC	F: CAATGTGTCCGTCGTGGATCT R: GTCCTCAGTGTAGCCCAAGATG

Table 2
Primers used for quantitative real-time PCR.

Name	Primer sequence (5′–3′)	Accession number	Product size (bp)
IL-1β	F:GAGGACATGAGCACCTTCTTT R:GCCTGTAGTGCAGTTGTCTAA	NM_008361.3	121
TNF-α	F:TTGTCTACTCCCAGGTTCTCT R: GAGGTTGACTTTCTCCTGGTATG	NM_013693.3	107
IL-6	F:CTTCCATCCAGTTGCCTTCT R:CTCCGACTTGTGAAGTGGTATAG	NM_001314054.1	134
GAPDH	F:CAATGTGTCCGTCGTGGATCT R:GTCCTCAGTGTAGCCCAAGATG	NM_001289726.1	124
MyD88	F:AGCAACTAGGACTGCCTTTC R:GAACTCTTCCACTCAGCTATCC	NM_010851.2	142

2.12. Western blotting assay

Total protein was extracted from lung tissues and treated cells which were lysated by the RIPA reagent (Biosharp, China) according to the manufacturer's instructions. The total protein concentration was determined with a BCA protein assay kit (Thermo Scientific, MA, USA). After the amount of protein samples in each group was consistently adjusted to 40 μg, proteins were separated using 12% SDS-PAGE and transferred onto polyvinylidinedifluoride (PVDF) membranes (Millipore, USA). The membranes were blocked with 5% nonfat milk in TBST for 2 h and incubated at 4 °C overnight with primary antibodies (1:1000 dilutions). Blots were washed and incubated with the appropriate HRP-conjugate secondary antibody (1:4000 dilutions) for 2 h. Proteins were detected using an enhanced chemiluminescence kit, and the intensities were quantified using Image J gel analysis software.

2.13. RNA extraction and RT-qPCR analysis

Total RNA was extracted from the lung tissues and cells using Trizol (Invitrogen, USA). Total RNA was reverse transcribed into complementary DNA (cDNA) using the PrimeScript RT reagent Kit and miRNA Reverse Transcription System TaqMan MicroRNA assay (Applied Biosystems, Foster City, USA) followed by the standard protocols, respectively. To detect miR-128 expression, cDNA was synthesized using a miR-128-specific stem-loop primer. Three replicates were set for each sample. The expression level of each gene was normalized to the threshold cycle (CT) value of the corresponding Glyceraldehyde-3-phosphate dehydrogenase (GAPDH) using the $2^{-\Delta\Delta Ct}$ comparative method. The Primer Premier software (PREMIER Biosoft International, Palo Alto, California, USA) was used to design specific primers for genes needed for research based on known sequences (Table 2).

2.14. Plasmid constructs and luciferase reporter assay

For the miRNA-target analysis, the fragment of the MyD88 mRNA 3′UTR was amplified from the mice genomic DNA using specific primers (Table 2). The amplified fragments containing wild-type were inserted into a psiCHECK™-2 reporter vector (Promega, Madison, WI, United States) using *Xho*I and *Not*I to construct a WT-3′UTR (WT-psiCHECK™-2/MyD88 3′UTR) luciferase reporter vector. The authenticity of synthetic WT-3′UTR was confirmed for sequencing by the company (Genecreate, Wuhan, China). Additionally, we obtained MuT-3′UTR, a psiCHECK-2 luciferase reporter vector containing the mutant 3′UTR of MyD88 sharing a 7-bp deletion in the conserved miR-128 binding site, from Shanghai Generay Biotech. WT-3′UTR or MuT-3′UTR reporter plasmids (200 ng) were co-transfected with the miR-128 mimic or the negative control of miR-128 mimic into 293T cells using Lipofectamine 2000™. After 24 h, the cells were lysed, and reporter activity was assessed using the dual luciferase reporter assay system (Promega, Madison, WI, USA).

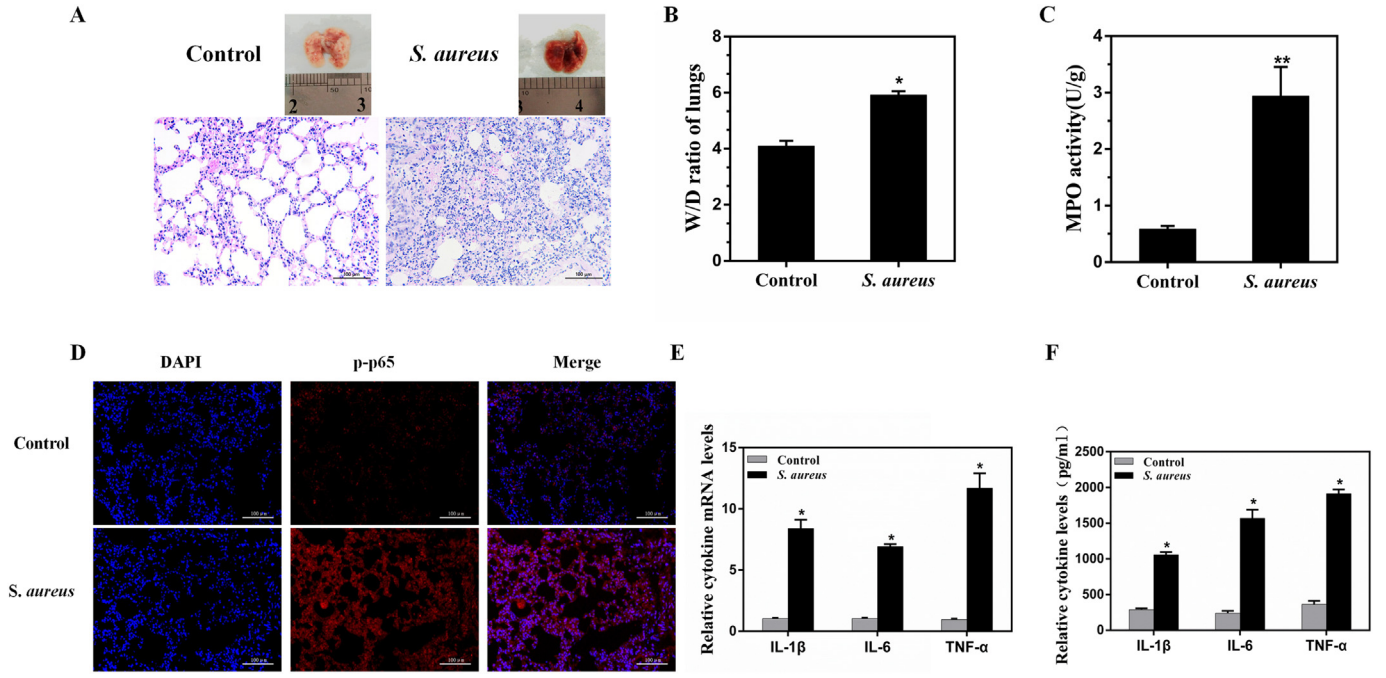

Fig. 1. *S. aureus* induces ALI in mice. (A) Histopathology of lung tissues after *S. aureus* stimulation (HE, ×200), scale bar = 100 μm. Mice were intratracheally administered with *S. aureus* for 24 h (n = 3). (B) W/D ratio of lungs (n = 3). (C) The infiltration of neutrophils in the lung tissues was determined by MPO activity (n = 3). (D) Translocation of the p65 subunit from the cytoplasm into the nuclei was evaluated by immunofluorescence. Blue spots represent cell nuclei, and red spots represent p-p65 staining (n = 3). Scale bar = 100 μm. (E, F) The concentration of IL-1β, IL-6 and TNF-α at mRNA and protein levels were measured by qPCR and ELISA for assessing the extent of inflammation in lung tissues (n = 6). GAPDH was used as a control. Control, the control group without *S. aureus* infection; *S. aureus*, *S. aureus* stimulation group. Data are expressed as the mean ± S.D. of three independent experiments. *P < 0.05; **P < 0.01 (Student's *t*-test). (For interpretation of the references to color in this figure legend, the reader is referred to the web version of this article.)

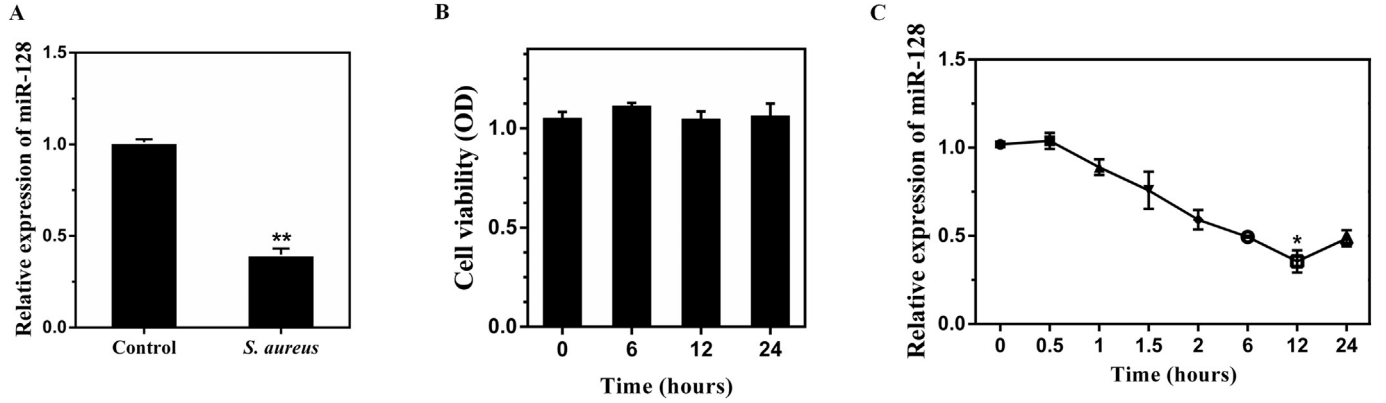

Fig. 2. *S. aureus* down-regulates miR-128 expression in lung tissues of mice and RAW 264.7 macrophages. (A) MiR-128 was detected in the lung tissues of *S. aureus* treated mice by qPCR. (B) The effects of inactivated *S. aureus* on the viability of RAW264.7 cells. Cell viability was determined with a CCK-8 assay kit. (C) Cells were stimulated with inactivated *S. aureus* (MOI = 10) for 0, 0.5, 1, 1.5, 2, 6, 12, and 24 h. The expression level of miR-128 was measured by qPCR. U6 snRNA was used as an endogenous control. The data are presented as the mean ± S.D. of three independent experiments. *P < 0.05; **P < 0.01 (Student's *t*-test).

2.15. Small interfering RNA

At 70–80% confluence, the cells were inoculated in 6-well plates and were transfected with 100 nM siRNA duplexes using Lipofectamine 2000™ for 24 h, followed by inactivated *S. aureus* infection according to the standard protocol. MyD88 siRNA or its negative control RNA (si-NC) was from GenePharma. The transfection efficiency was examined with a fluorescence microscope, and the cells were harvested for protein and RNA extraction.

2.16. Statistical analysis

All experiments were repeated three times. Data was presented as the mean ± S.D. Statistical significance was determined by Student's *t*-test, with a probability value of < 0.05 was considered to be statistically significant.

3. Results

3.1. S. aureus induces ALI in mice

The possible role of miR-128 in ALI in mice was studied by giving intra-nasal *S. aureus* stimulation. Morphologically appearance (Fig. 1A) showed visual swelling and congestion compared with the control group. H&E staining of lung section also showed pronounced manifestation of the alveolar wall, congestion and edema. Further W/D ratio

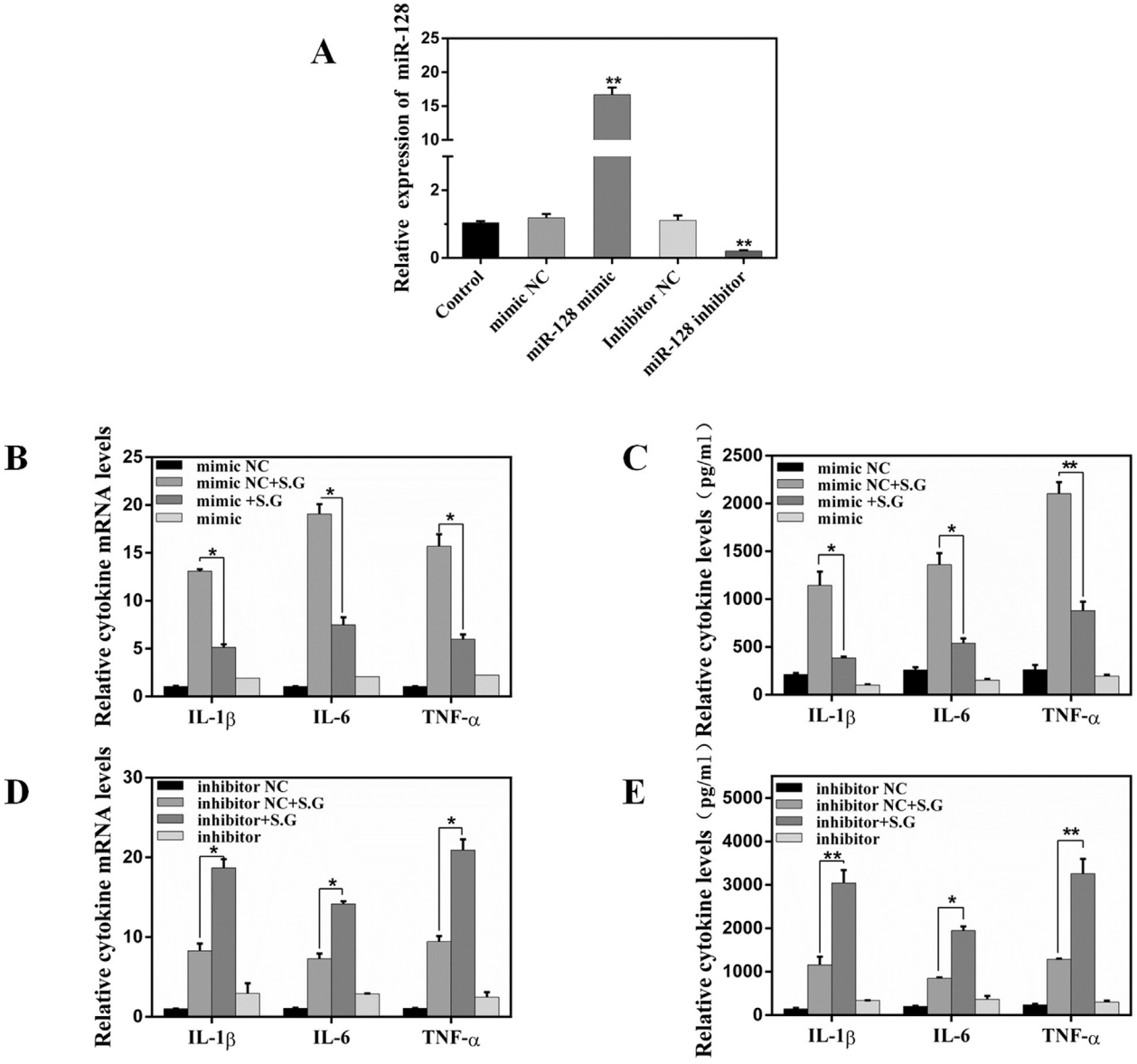

Fig. 3. MiR-128 inhibits *S. aureus*-induced inflammatory cytokines production. (A) After cells were teansfected with the miR-128 mimic, the miR-128 inhibitor or their negative control duplexes (NC), cells were cultured for 24 h. RT-qPCR was performed to assess miR-128 expression. (B) Cells were transfected with the miR-128 mimic or its negative control duplex. After 24 h, cells were treated with inactivated *S. aureus* (MOI = 10) for another 12 h. The mRNA levels were measured by qPCR. (C) After cells were treated as described in (B), the protein levels were measured by an ELISA. (D) Cells were transfected with the miR-128 inhibitor or its negative control duplex. The cells were treated and the mRNA levels were measured as described in (B). (E) After cells were treated as described in (D), the protein levels were measured by ELISA. S.G, treatment with *S. aureus*. Data are presented as the mean ± S.D. of three independent experiments. *P < 0.05; **P < 0.01 (Student's *t*-test).

was obtained by weighting the dry and wet lungs of each group. The *S. aureus* infected group showed significantly increased W/D ratio (Fig. 1B) and MPO activity (Fig. 1C). NF-κB p65, a major member of NF-κB (component of one of the main pathways in which cytokines are activated in inflammatory response), is activated by *S. aureus* to induce IL-1β, IL-6 and TNF-α (Fig. 1D). IL-1β, IL-6 and TNF-α mRNA and protein expression levels in *S. aureus*-stimulated lung tissues were highly up-regulated relative to the control Group (Fig. 1E–F). The results showed that *S. aureus* is responsible for mice lungs inflammation.

3.2. S. aureus down-regulates miR-128 expression in lung tissues of mice and RAW 264.7 cells

Previous studies showed that lots of miRNAs induced by *S. aureus* regulate inflammatory response [21]. Our RT-qPCR results showed a significant reduction in miRNA-128 in *S. aureus* infected mice group as compared with the control group (Fig. 2A). In order to further explore the change in miR-128 expression in RAW264.7 macrophages, we first examined whether inactivated *S. aureus* could have cytotoxic effects on RAW264.7 cells with the CCK-8 assay. The results showed that macrophage viability was not affected by inactivated *S. aureus* at MOI of 10 (Fig. 2B). Thus, RAW264.7 cells were stimulated with inactivated *S. aureus* at different time points. The results showed a dramatical decrease in miR-128 expression after treatment with *S. aureus* (MOI = 10) until 12 h in a time-dependent manner (Fig. 2C). Taken together, these data indicated that *S. aureus* down-regulates miR-128 levels in *S. aureus*-induced ALI mice and *S. aureus*-treated RAW264.7 cells, which suggest the involvement of miR-128 in *S. aureus*-mediated immune responses.

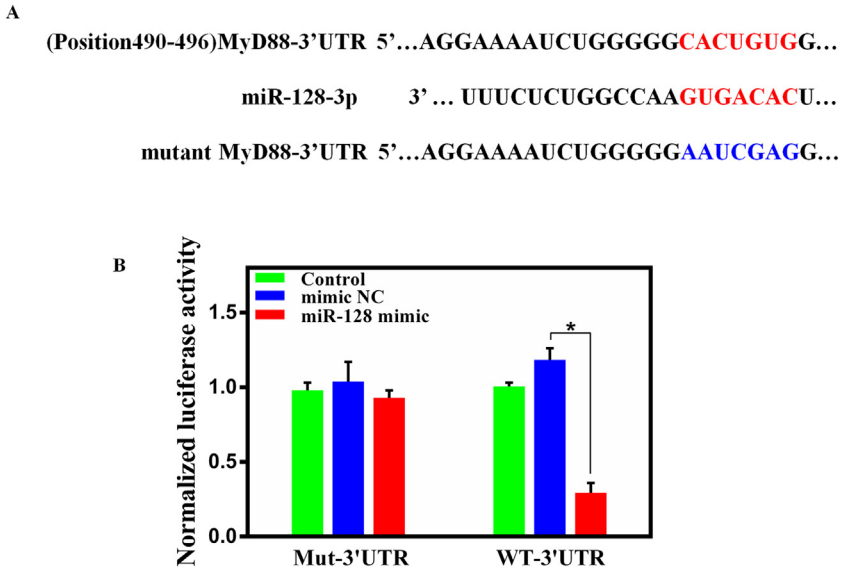

Fig. 4. MiR-128 regulates MyD88 expression by directly targeting its 3′UTR. (A) The alignment of miR-128 and its target site in the 3′UTR of MyD88, as detected by TargetScan. Mutant MyD88 3′-UTR included several mutation (blue letters) in miR-128 binding site. (B) 293T cells were co-transfected with the wild- (WT-3′UTR) or mutant-type MyD88 3′-UTR (Mut-3′UTR) luciferase reporter vector, together with miR-128 mimic or its negative control duplex (NC) whose final concentration was 20 nM as indicated. After 24 h, firefly luciferase activity was measured and normalized to Renilla luciferase activity. Data are presented as the mean ± S.D. of three independent experiments. *P < 0.05 (Student's *t*-test). (For interpretation of the references to color in this figure legend, the reader is referred to the web version of this article.)

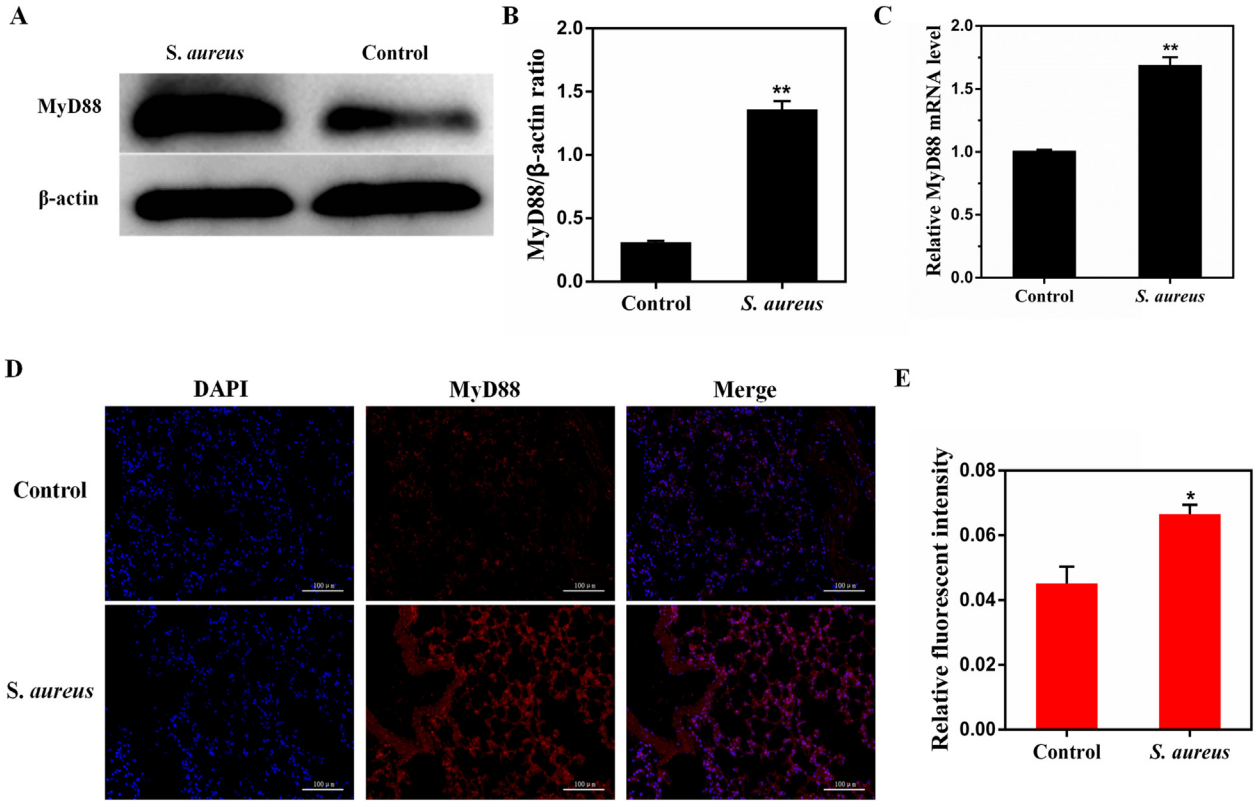

Fig. 5. MyD88 expression inversely correlates with miR-128 expression in vivo. (A) The protein level of MyD88 was detected by WB. β-Actin was used as an internal control. (B) Gray values of MyD88 protein were measured by IPP software. (C) The mRNA level of MyD88 was detected by qPCR. GAPDH was used as an internal control. (D) Immunofluorescence staining was performed to identify the expression of MyD88 (×200), scale bar = 100 μm. Blue spots represent cell nuclei, and red spots indicate MyD88 staining. (E) The intensity of MyD88. Values are given as the mean ± S.D. of three experiments. *P < 0.05 (Student's *t*-test). (For interpretation of the references to color in this figure legend, the reader is referred to the web version of this article.)

3.3. MiR-128 inhibits S. aureus-induced inflammatory cytokines production

To further confirm the effect of miR-128 on the secretion of inflammatory mediators. RAW264.7 cells were transfected with the miR-128 mimic or the inhibitor of miR-128 to overexpress or inhibit the expression of miR-128. After transfection, samples were collected and the mRNA level of miR-128 was analyzed by qPCR. It was found that the expression level of miR-128 after transfection of the mimic was increased more than 10 times higher compared to that of the untransfected mimic. (Fig. 3A). Moreover, after transfection with miR-128 mimic, the levels of IL-1β, IL-6 and TNF-α were significantly lowered in RAW264.7 cells treated with inactived *S. aureus* (Fig. 3B and C). However, when the miR-128 inhibitor was transfected, the opposite results were obtained (Fig. 3D and E). These data indicated that miR-128 down-regulates the levels of pro-inflammatory cytokines.

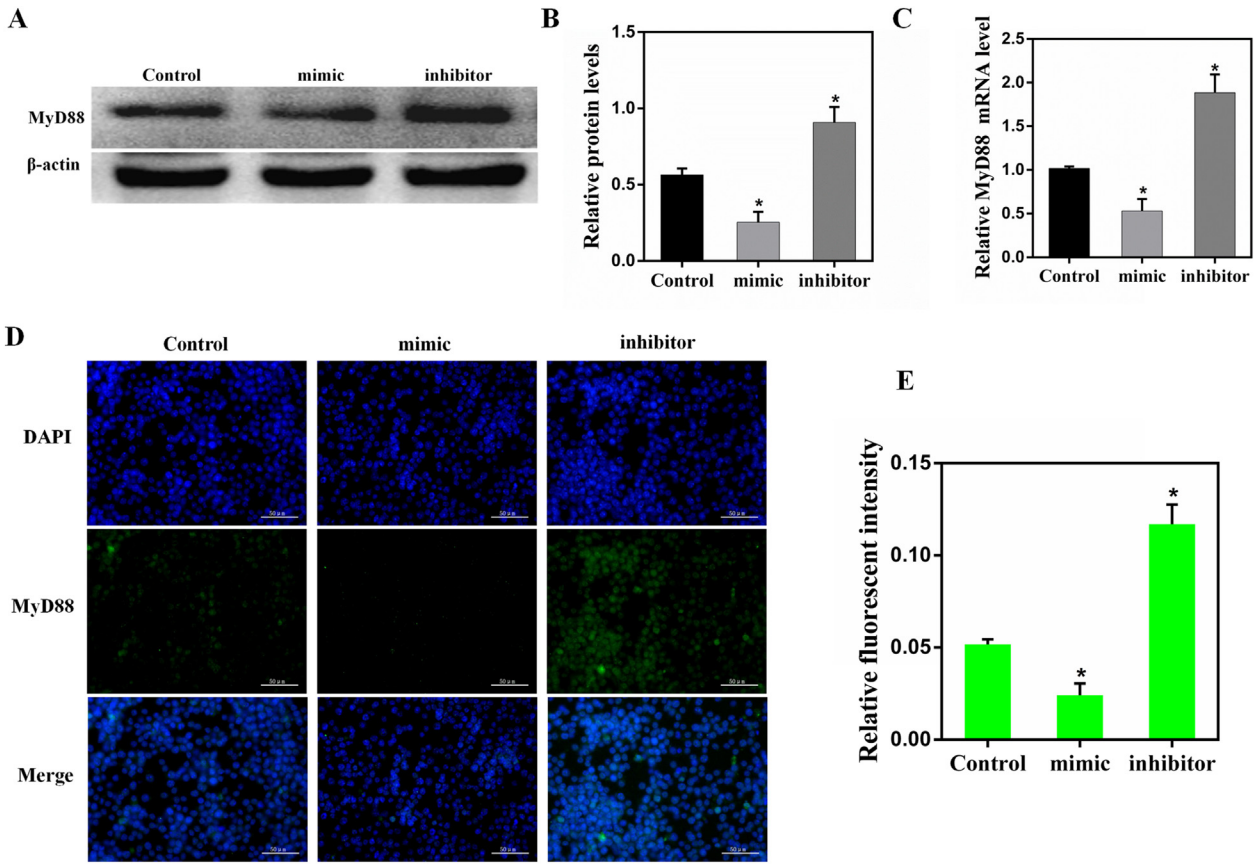

Fig. 6. MyD88 expression inversely correlates with miR-128 expression in vitro. Cells were transfected with the miR-128 mimic, the miR-128 inhibitor or their negative control duplexes for 48 h. (A) The protein levels of MyD88 were detected by WB. β-Actin was used as an internal control. (B) Gray values of MyD88 protein were measured by IPP software. (C) The mRNA level of MyD88 was detected by qPCR. GAPDH was used as an internal control. (D) Immunofluorescence staining was performed to identify the expression of MyD88 (×400), scale bar = 50 μm. Blue spots represent cell nuclei, and green spots indicate MyD88 staining. (E) The intensity of MyD88. Values are given as the mean ± S.D. of three experiments. *P < 0.05 (Student's *t*-test). (For interpretation of the references to color in this figure legend, the reader is referred to the web version of this article.)

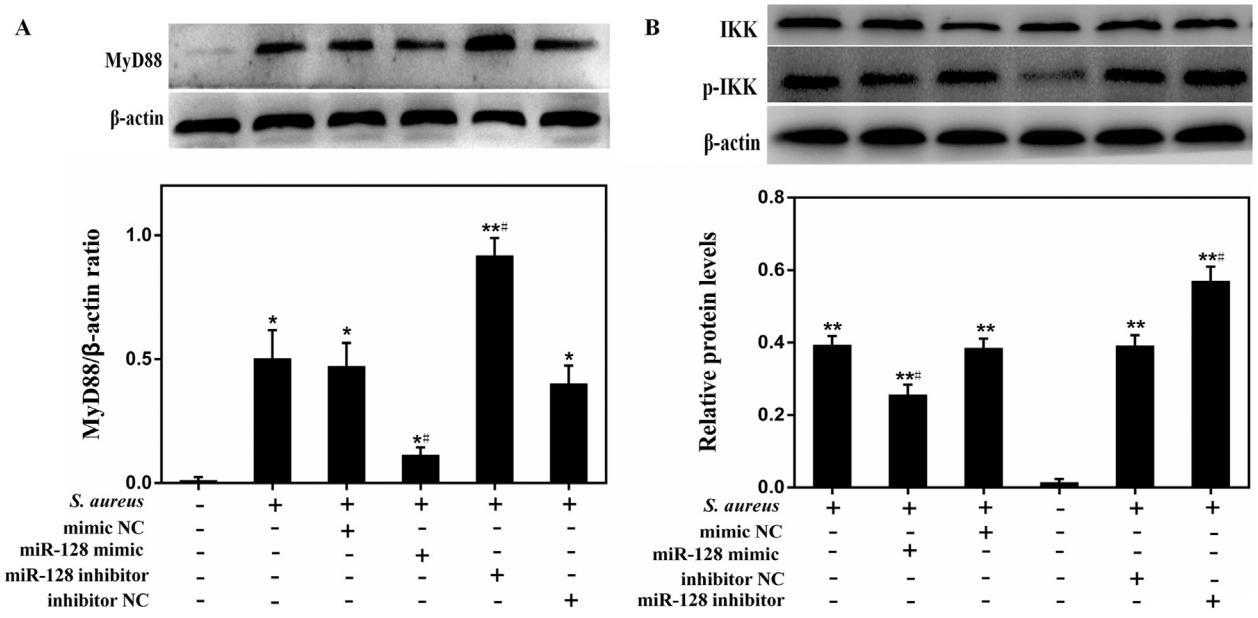

Fig. 7. MiR-128 downregulates the expression level of Myd88 and p-IKK of NF-κB pathway in *S. aureus*-stimulated RAW264.7 cells. Cells were transfected with the miR-128 mimic, the miR-128 inhibitor, or their negative control duplexes (NC) for 24 h, then treated with inactivated *S. aureus* (MOI = 10) for another 12 h. The expression of MyD88 and p-IKK (p-pIKKα/β) were determined using WB. β-Actin was used as a control. Gray values of the indicated proteins were measured by Image-Pro Plus (IPP) 6.0 software. (A) MyD88. (B) p-IKK (p-pIKKα/β). Data are expressed as the mean ± S.D. of three independent experiments. *P < 0.05; **P < 0.01 versus the control group; #P < 0.05, ##P < 0.01 versus the *S. aureus* group (Student's *t*-test).

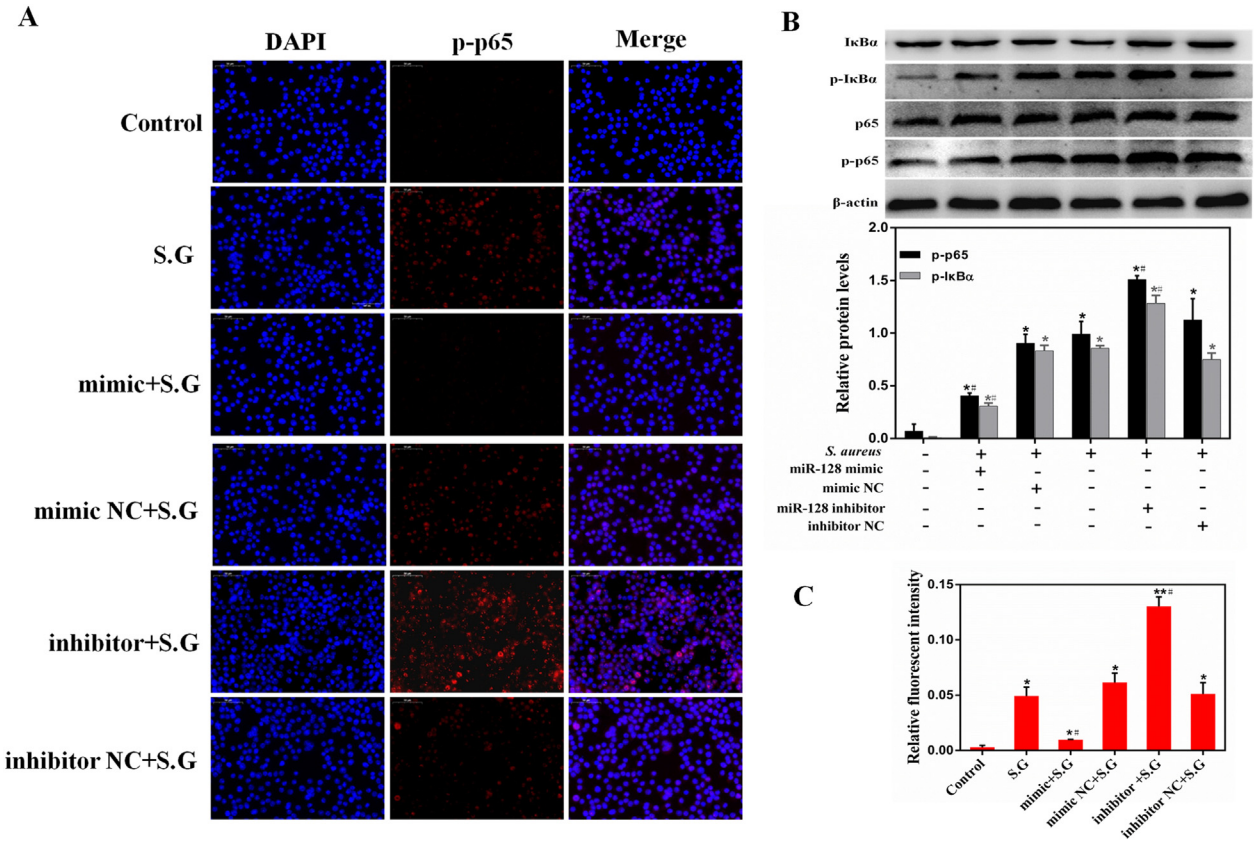

Fig. 8. MiR-128 inhibits *S. aureus*-induced activation of NF-κB signaling. Cells were treated as Fig. 7. (A) Translocation of the p65 subunit from the cytoplasm into the nuclei was evaluated with immunofluorescence (×400). Blue spots represent cell nuclei, and red spots represent p-p65 staining; scale bar = 50 μm. (B) The expression of p-p65 and p-IκBα was determined using WB. β-Actin was used as a control. Gray values of the indicated proteins were measured by Image-Pro Plus (IPP) 6.0 software. (C) The integrated option density (IOD) of DAPI was used as an internal control. The IOD and area of cells were measured by IPP 6.0 software, and the fluorescence intensity of p-p65 was expressed as IOD/area. S.G, treatment with *S. aureus*. Data are expressed as the mean ± S.D. of three independent experiments. *P < 0.05; **P < 0.01 versus the control group; #P < 0.05, ##P < 0.01 versus the *S. aureus* group (Student's *t*-test). (For interpretation of the references to color in this figure legend, the reader is referred to the web version of this article.)

3.4. MiR-128 regulates MyD88 expression by directly targeting its 3′UTR

To investigate the biological function and regulatory mechanisms of miR-128 in *S. aureus*-treated RAW264.7 cells, its putative target was predicted. Among all the many putative targets, we eventually filtered out MyD88 related to inflammation as the target for miR-128 in the study. Fig. 4A shows a putative target seed sequence. Subsequently, luciferase reporter assay was performed to determine whether MyD88 was a direct target of miR-128. MyD88 WT-3′UTR or MuT-3′UTR was co-transfected with the miR-128 mimic or its negative control mimic (mimic NC) into the 293T cells. As shown in Fig. 4B, the luciferase activity of MyD88 WT-3′UTR was significantly decreased in cells transfected with the miR-128 mimic. However, the luciferase activity of MyD88 MuT-3′UTR had no notable difference between cells transfected with the miR-128 mimic and the mimic NC. These data indicated that miR-128 regulates MyD88 expression by directly targeting the 3′UTR of MyD88 mRNA.

3.5. MyD88 expression inversely correlates with miR-128 expression

MyD88 is a key downstream adaptor molecule for most Toll-like receptors and interleukin-1 receptors [31]. To further determine the relationship between miR-128 and MyD88, the expression of MyD88 were examined using WB, qPCR and immunofluorescence in vivo (Fig. 5A–E) and in vitro (Fig. 6A–E). It was found that miR-128 not only lowered MyD88 mRNA level but also down-regulated the protein level of MyD88. In conjunction with Figs. 2A and 3A, MyD88 expression inversely correlates with miR-128 expression, suggesting that miR-128 may directly function at the MyD88 mRNA level and then affect its translation.

3.6. MiR-128 inhibits S. aureus-induced activation of NF-κB signaling

Lipopolypeptides in *S. aureus* that is widely present on the surface of gram-positive bacteria can activate downstream NF-κB signaling pathways through TLR2 [26,27]. It is confirmed that many molecules involved in the early stages of immune response and inflammatory reactions are regulated by NF-κB [28]. Therefore, we speculated that miR-128 may be involved in NF-κB signaling pathway to regulate the development of inflammation.

To further verify the specific role of miR-128 in *S. aureus* inflammatory response, the miR-128 mimic was transfected into RAW264.7 cells and the transfectants were stimulated with inactivated *S. aureus* for 12 h. MyD88 and IKK, upstream components of NF-κB signaling, were detected. WB showed that levels of MyD88 and p-IKK were significantly suppressed (Fig. 7A–B). Meanwhile, the results showed that the phosphorylation levels of p65 and IκBα were markedly inhibited in cells transfected with the miR-128 mimic (Fig. 8B). Fig. 8A and C showed that the miR-128 mimic inhibited the nuclei import of NF-κB p65. Our data show that miR-128 inhibits the expression of MyD88 and the activation of the NF-κB signaling, which in turn suppresses the inflammatory response.

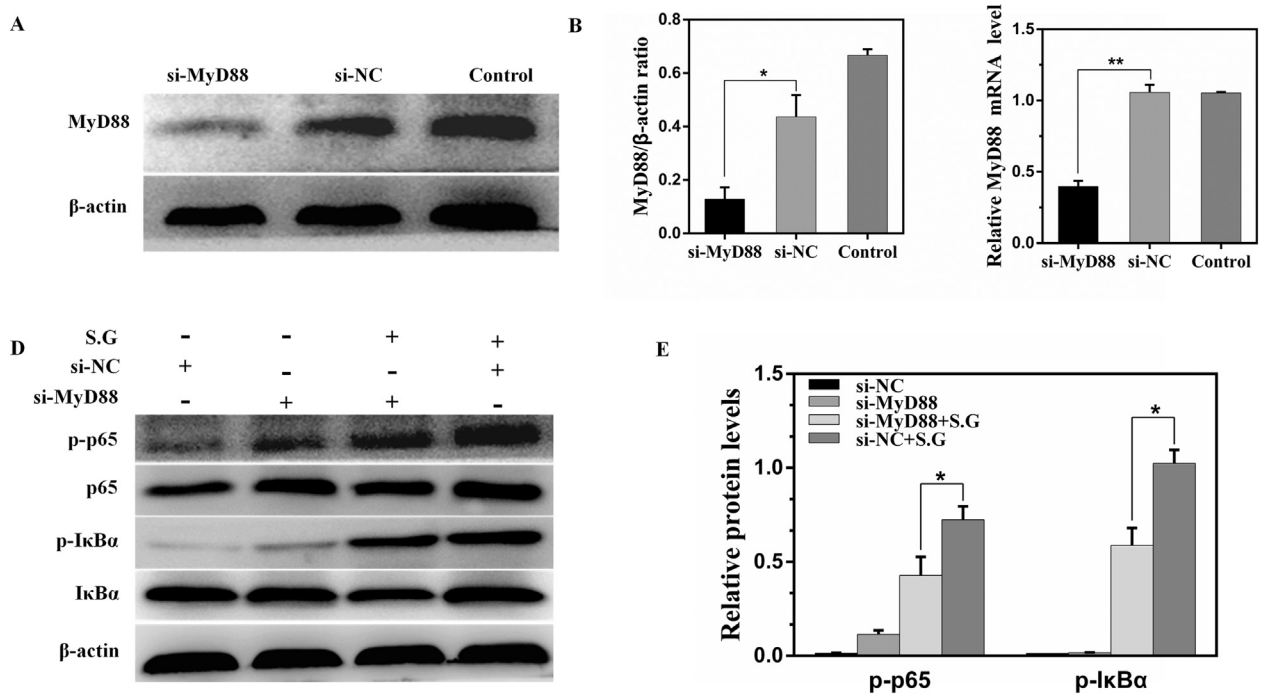

Fig. 9. Knockdown of MyD88 inhibits the phosphorylation of NF-κB p65 and IκBα in RAW264.7 cells. (A, B, C) After 48 h of transfection with control siRNA (Si-NC) or MyD88 siRNA (Si-MyD88) at doses of 200 nM, WB and qPCR were used to analyze the MyD88 protein and mRNA expression, respectively, in RAW264.7 cells. (D) Cells were transfected with 200 nM Si-MyD88 or Si-NC for 24 h, and then stimulated with inactivated *S. aureus* (MOI = 10) for 12 h. The protein levels of NF-κB p65 and p-IκBα were measured by WB. Protein expression was normalized with β-actin. (E) Gray values of the indicated proteins were measured by IPP 6.0 software. NC, negative control duplex; S.G, treatment with *S. aureus*. Data are expressed as the mean ± S.D. of three independent experiments. *P < 0.05; **P < 0.01(Student's *t*-test).

3.7. Knockdown MyD88 inhibites S. aureus-induced inflammation in RAW264.7 cells

To confirm the mechanisms by which miR-128 regulates *S. aureus*-triggered proinflammatory cytokine production, RAW264.7 cells were transfected with MyD88 siRNA to knock down the expression of MyD88. The mRNA and protein levels of MyD88 were significantly suppressed after treatment with MyD88 siRNA compared to RAW264.7 cells treated with MyD88 si-NC (Fig. 9A–C). The immunostaining for p-p65 revealed that MyD88 siRNA blocked the translocation of NF-κB from the cytosol to the nuclei (Fig. 10A–B). WB results (Fig. 9D–E) also showed that when RAW264.7 cells were incubated with *S. aureus* for 12 h, silencing MyD88 markedly reduced the levels of p-p65 and p-IκBα and inhibited the *S. aureus*-triggered IL-1β, IL-6 and TNF-α production at both the mRNA and the protein levels (Fig. 10C),which are similar effects to those observed in macrophages overexpressing miR-128. These results suggest that MyD88 plays an essential role in regulating the effect of *S. aureus* on the production of proinflammatory cytokines.

4. Discussion

ALI is a common clinical syndrome. Bacterial infections are the leading cause of ALI. A number of studies have shown that finger peptides widely presenting on the surface of gram-positive bacteria can activate NF-κB signaling pathway through TLR2, and NF-κB can induce excessive or sustained expression of cytokines IL-1β, IL-6 and TNF-α [26]. Therefore, the levels of IL-1β, IL-6 and TNF-α were detected in lung tissues of ALI and cells induced by *S. aureus*. As expected, the results showed that IL-1β, IL-6 and TNF-α were significantly up-regulated in the *S. aureus* group and that NF-κB was also translocated into the nuclei, further confirming inflammation caused by *S. aureus*.

It is very important to clarify the development of ALI because of its high mortality rate, high damage and more use of antibiotics [3]. The role of miR-128 in inflammation has also been studied, but it is still not clear. Here, we found that miR-128 expression was significantly decreased in *S. aureus*-induced ALI and *S. aureus*-treated RAW264.7 macrophages. Our results demonstrated that miR-128 targets the 3′UTR of MyD88 and negatively regulates the activation of NF-κB signaling by *S. aureus*, reducing the production of pro-inflammatory cytokines. Therefore, miR-128 may be a new target for preventing *S. aureus*-induced inflammation.

TLR activation affects the expression of some key miRNAs under *S. aureus* stimulation [32–36]. Shyamasundar et al. [30] revealed that miR-128 could be increased during LPS-induced inflammation and overexpression of miR-128 enhanced expression of genes associated with inflammation, pro-inflammatory cytokines. Conversely, miR-128 has been demonstrated to have an anti-inflammatory effect in regulating LPS-stimulated macrophages [22]. It seems that a specific miRNA is inconsistent in different physiological and pathological conditions and plays different roles, presumably because of the targeted diversity of miRNA-mRNA interactions. Our results revealed that overexpression of miR-128 by the miR-128 mimic inhibited *S. aureus*-induced macrophage inflammation, but inhibition of miR-128 expression by the miR-128 inhibitor significantly increased *S. aureus*-induced inflammatory responses. These results indicated that inhibition of macrophage hyper-inflammatory activity is a mechanism involved in the up-regulated expression of miR-128 and protection against ALI.

Although many target genes for miR-128 are predicted by online sites, some target genes may not respond to miRNAs. To date, some genes including many protein receptors, extracellular matrix glycoprotein and kinases have been experimentally validated to be a target of miR-128 [37–39]. After searching integrating multiple online prediction sites, MyD88 mRNA was predicted to be a candidate molecular target of miR-128. We found that miR-128 regulates the inflammatory response by regulating MyD88.

The miRNAs represent a novel pathway for post-transcriptional

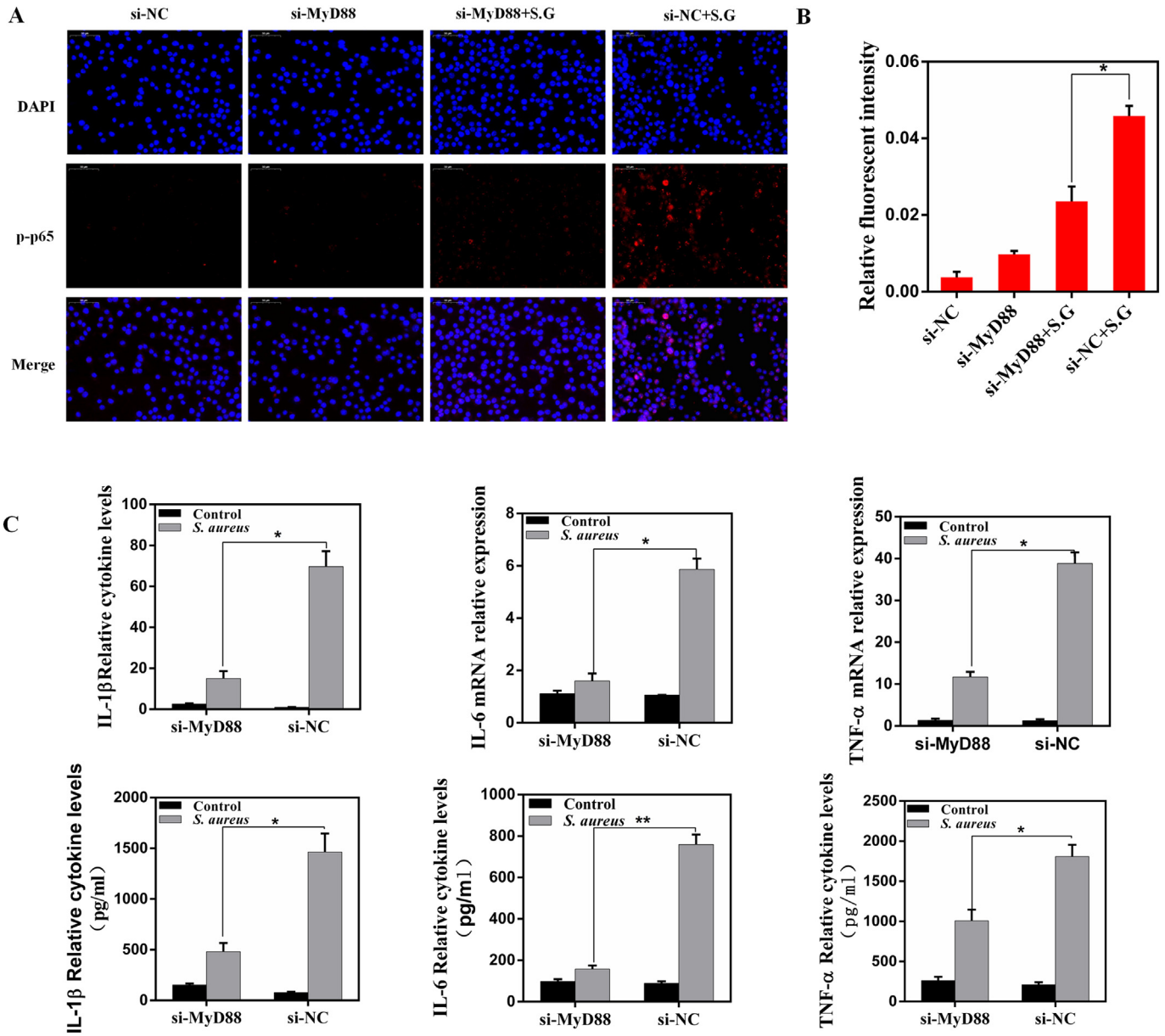

Fig. 10. Knockdown of MyD88 alleviates *S. aureus*-induced inflammation in RAW264.7 cells. Cells were transfected with 200 nM Si-MyD88 or Si-NC for 24 h, and then stimulated with inactivated *S. aureus* (MOI = 10) for 12 h. (A) Translocation of the p65 subunit from the cytoplasm into the nuclei was evaluated with immunofluorescence (×400). Blue spots represent cell nuclei, and red spots represent p-p65 staining; scale bar = 50 μm. (B) The fluorescence intensity of p-p65. (C) The levels of the cytokines IL-1β, IL-6 and TNF-α were determined with an ELISA and qPCR. GAPDH was used as a control. NC, negative control duplex; S.G, treatment with *S. aureus*. Data are expressed as the mean ± S.D. of three independent experiments. *P < 0.05; **P < 0.01(Student's *t*-test). (For interpretation of the references to color in this figure legend, the reader is referred to the web version of this article.)

regulation of gene expression, by blocking translation or inducing degradation of target mRNAs. This process has been proposed to be the major controlling mechanism by tissue- and cell type-specific expression of miRNAs [7]. In this report, MyD88 mRNA was confirmed to be a molecular target of miR-128 by dual luciferase reporter assay. When 293T cells were co-transfected with the miR-128 mimic and the WT-3′UTR MyD88 plasmid, luciferase expression was significantly reduced, while no significant modulation was observed with Mut-3′UTR. These results indicate that miR-128 can interact with the 3′UTR of MyD88 mRNA and effectively inhibit its translation. RT-qPCR and WB results further support this hypothesis. All of these data strongly suggest that MyD88 is a target for miR-128 after *S. aureus* stimulation.

MyD88 is a general adaptor protein that plays a crucial role in the Toll/IL-1 receptor family signalings [24]. To further confirm the role of MyD88 in *S. aureus*-induced inflammatory responses, we also transfected MyD88 siRNA into macrophages followed by incubation with *S. aureus*. The treatment significantly reduces the secretion of inflammatory factors and suppresses the occurrence of inflammatory reactions by inhibiting the activation of IκBα and p65. In this report, the results of RNA interference indicated that overexpression of miR-128 can negatively regulate *S. aureus*-induced proinflammatory cytokines IL-1β, IL-6 and TNF-α via targeting MyD88.

It is well known that each individual miRNA has the ability to regulate multiple genes. The role between them is network-like. MyD88 is not the only target for miR-128 to exert anti-inflammatory effects. A number of studies have previously confirmed that MyD88 is a target for multiple miRNAs [40–44], and that miR-128 also has multiple different targets under complex pathological conditions [25,30,45]. Thus miRNA function was found to be more diverse in case of *S. aureus* infection. In our research, regulation of MyD88 was indeed the major mechanism of

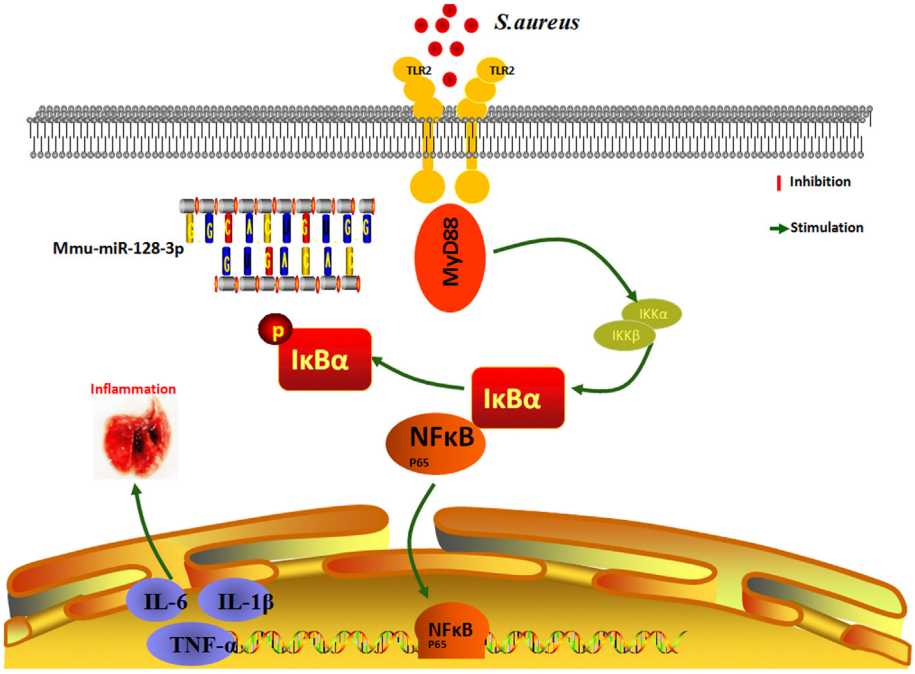

Fig. 11. Schematic diagram depicting the signaling pathways for miR-128 in the regulation of *S. aureus*-triggered inflammatory responses in macrophages. P, phosphorylation.

miR-128 in *S. aureus*-induced inflammation and miR-128 may be a direction and target for the treatment of *S. aureus*-associated inflammation.

In summary, the study provided the first evidence that miR-128 inhibits the inflammatory activity of macrophages during *S. aureus*-induced ALI by suppressing MyD88. MiR-128-mediated post-transcriptional regulation can potentially be involved in fine-tuning *S. aureus*-TLR2-induced inflammatory response in macrophages. MiR-128 was down-regulated upon infection of *S. aureus*, and then the decreased miR-128 enhanced the TLR2-triggered NF-κB pathways through binding the target 3′UTR MyD88 at the posttranscriptional level, consequently causing the down-regulation of proinflammatory cytokine production, thereby exerting its anti-inflammatory effects. This is a positive loop in which the *S. aureus*-TLR2-triggered inflammatory response is tightly controlled via the TLR2-MyD88-NF-κB pathway (Fig. 11). Therefore, miR-128 is likely to be used in the treatment approach in inflammatory diseases caused by *S. aureus* infection.

Funding

This study was supported by the National Natural Science Foundation of China (NO. 31272631, 31472254).

Author contributions

XM and GZ conceived and designed the experiments. XM, SG, and YY carried out the experiments. KJ and XW analyzed the data. XM and AZ wrote the manuscript. All authors agreed to be responsible for the content of the work.

Conflict of interest statement

The authors declare that the research was conducted in the absence of any commercial or financial relationships that could be construed as a potential conflict of interest.

References

[1] A.M. Modrykamien, P. Gupta, The acute respiratory distress syndrome, JAMA 307 (23) (2012) 2542.
[2] G.D. Rubenfeld, et al., Incidence and outcomes of acute lung injury, N. Engl. J. Med. 353 (2) (2005) 1685–1693.
[3] H. Yao, et al., Protective effects of dioscin against lipopolysaccharide-induced acute lung injury through inhibition of oxidative stress and inflammation, Front. Pharmacol. 8 (30704) (2017).
[4] K. Tsushima, et al., Acute lung injury review, Intern. Med. 48 (9) (2009) 621.
[5] H. Yao, et al., Protective effects of dioscin against lipopolysaccharide-induced acute lung injury through inhibition of oxidative stress and inflammation, Front. Pharmacol. 8 (30704) (2017).
[6] R.M. Sweeney, M. Griffiths, D. Mcauley, Treatment of acute lung injury: current and emerging pharmacological therapies, Semin. Respir. Crit. Care Med. 34 (4) (2013) 487–498.
[7] J. Krol, I. Loedige, W. Filipowicz, The widespread regulation of microRNA biogenesis, function and decay, Nat. Rev. Genet. 11 (9) (2010) 597–610.
[8] F. Meisgen, et al., MiR-146a negatively regulates TLR2-induced inflammatory responses in keratinocytes, J. Investig. Dermatol. 134 (7) (2014) 1931–1940.
[9] B. Xiao, et al., Induction of microRNA-155 during *Helicobacter pylori* infection and its negative regulatory role in the inflammatory response, J. Infect. Dis. 200 (6) (2009) 916–925.
[10] X. Tang, G. Tang, S. Ozcan, Role of microRNAs in diabetes, Biochim. Biophys. Acta 1779 (11) (2008) 697–701.
[11] R. Liu, et al., FOXP3 controls an miR-146/NF-Î°B negative feedback loop that inhibits apoptosis in breast cancer cells, Cancer Res. 75 (8) (2015) 1703–1713.
[12] Y. Peng, et al., The crosstalk between microRNAs and the Wnt/β-catenin signaling pathway in cancer, Oncotarget 8 (8) (2016).
[13] P.M. Voorhoeve, et al., A genetic screen implicates miRNA-372 and miRNA-373 as oncogenes in testicular germ cell tumors, Oxygen Transport to Tissue XXXIII, 124(6) 2006, pp. 17–46.
[14] K.M. Pauley, S. Cha, E.K.L. Chan, MicroRNA in autoimmunity and autoimmune diseases, J. Autoimmun. 32 (3–4) (2009) 189–194.
[15] A.M. Ardekani, M.M. Naeini, The role of microRNAs in human diseases, Avicenna J. Med. Biotechnol. 2 (4) (2010) 161–179.
[16] C.H. Lawrie, et al., Detection of elevated levels of tumour-associated microRNAs in serum of patients with diffuse large B-cell lymphoma, Br. J. Haematol. 141 (5) (2008) 672–675.
[17] E. Sonkoly, et al., MicroRNAs: novel regulators involved in the pathogenesis of psoriasis? PLoS One 2 (7) (2007) e610.
[18] C.I. Caescu, et al., Colony stimulating factor-1 receptor signaling networks inhibit mouse macrophage inflammatory responses by induction of microRNA-21, Blood 125 (8) (2015) e1.
[19] Y. Zhao, et al., MicroRNA-124 promotes intestinal inflammation by targeting aryl hydrocarbon receptor in Crohn's disease, J. Crohn's Colitis 10 (6) (2016) 703–712.
[20] S. Banerjee, et al., miR-125a-5p regulates differential activation of macrophages and inflammation, J. Biol. Chem. 288 (49) (2013) 35428–35436.
[21] R. Rao, P. Nagarkatti, M. Nagarkatti, Role of miRNA in the regulation of

inflammatory genes in staphylococcal enterotoxin B-induced acute inflammatory lung injury and mortality, Toxicol. Sci. 144 (2) (2015) 284.
[22] H. Xiaokelaiti, et al., MiR-128-3p Regulates Inflammatory Response in LPS-stimulated Macrophages Through the TLR4-NF-κB Pathway, vol. 9, (2016), pp. 8005–8013.
[23] T.M.-N. Rocio, et al., MiR-18a, miR-27a, miR-128 and miR-155 Are Predicted to Target Inflammatory Pathways, (2014).
[24] C. Picard, et al., Pyogenic bacterial infections in humans with IRAK-4 deficiency, Science 321 (5889) (2008) 691–696.
[25] S. Wang, et al., Decreased miR-128 and increased miR-21 synergistically cause podocyte injury in sepsis, J. Nephrol. 30 (4) (2017) 1–8.
[26] T. Kawai, S. Akira, Signaling to NF-kappaB by Toll-like receptors, Trends Mol. Med. 13 (11) (2007) 460–469.
[27] F.D. Lowy, *Staphylococcus aureus* infections, N. Engl. J. Med. 339 (8) (1998) 520.
[28] J.P. Mitchell, R.J. Carmody, F. Loos (Ed.), Chapter Two - NF-κB and the Transcriptional Control of Inflammation, in International Review of Cell and Molecular Biology, Academic Press, 2018, pp. 41–84.
[29] H.S. Na, et al., Elevated miR-128 in periodontitis mitigates tumor necrosis factor-alpha response via P38 signaling pathway in macrophages, J. Periodontol. 87 (9) (2016) 1–18.
[30] S. Shyamasundar, et al., miR-128 regulates genes associated with inflammation and fibrosis of rat kidney cells in vitro, Anat. Rec. 301 (Suppl. 1) (2017).
[31] H.V. Bernuth, et al., Pyogenic bacterial infections in humans with MyD88 deficiency, Science 321 (5889) (2008) 691–696.
[32] F. Dilda, et al., *Escherichia coli* lipopolysaccharides and *Staphylococcus aureus* enterotoxin B differentially modulate inflammatory microRNAs in bovine monocytes, Vet. J. 192 (3) (2012) 514–516.
[33] T. Jin, et al., The role of microRNA, miR-24, and its target CHI3L1 in osteomyelitis caused by *Staphylococcus aureus*, J. Cell. Biochem. 116 (12) (2015) 2804–2813.
[34] W. Jin, et al., Transcriptome microRNA profiling of bovine mammary epithelial cells challenged with *Escherichia coli* or *Staphylococcus aureus* bacteria reveals pathogen directed microRNA expression profiles, BMC Genomics 15 (1) (2014) 181 ((2014-03-07). 15(1)).
[35] R. Modak, et al., Epigenetic response in mice mastitis: role of histone H3 acetylation and microRNA(s) in the regulation of host inflammatory gene expression during Staphylococcus aureus infection, Clin. Epigenetics 6 (1) (2014) 1–15.
[36] F. Xu, et al., Akt1-mediated regulation of macrophage polarization in a murine model of *Staphylococcus aureus* pulmonary infection, J. Infect. Dis. 208 (3) (2013) 528–538.
[37] Y. Zhu, et al., Reduced miR-128 in breast tumor-initiating cells induces chemotherapeutic resistance via Bmi-1 and ABCC5, Clin. Cancer Res. 17 (22) (2011) 7105–7115.
[38] C. Evangelisti, et al., MiR-128 up-regulation inhibits Reelin and DCX expression and reduces neuroblastoma cell motility and invasiveness, FASEB J. 23 (12) (2009) 4276–4287.
[39] J. Jiang, et al., MiR-128 reverses the gefitinib resistance of the lung cancer stem cells by inhibiting the c-met/PI3K/AKT pathway, Oncotarget 7 (45) (2016) 73188–73199.
[40] Y. Zhan, et al., MiRNA-149 modulates chemosensitivity of ovarian cancer A2780 cells to paclitaxel by targeting MyD88, J. Ovarian Res. 8 (1) (2015) 48 ((2015-07-30) 8(1)).
[41] G. Xu, et al., MicroRNA-149 negatively regulates TLR-triggered inflammatory response in macrophages by targeting MyD88, J. Cell. Biochem. 115 (5) (2014) 919.
[42] Z. Yang, et al., miR-203 protects microglia mediated brain injury by regulating inflammatory responses via feedback to MyD88 in ischemia, Mol. Immunol. 65 (2) (2015) 293–301.
[43] Q. Wu, et al., miR-489 inhibits silica-induced pulmonary fibrosis by targeting MyD88 and Smad3 and is negatively regulated by lncRNA CHRF, Sci. Rep. 6 (2016) 30921.
[44] B. Tang, et al., Identification of MyD88 as a novel target of miR-155, involved in negative regulation of *Helicobacter pylori*-induced inflammation, FEBS Lett. 584 (8) (2010) 1481–1486.
[45] Z. Rui, et al., MicroRNA-128-3p regulates mitomycin C-induced DNA damage response in lung cancer cells through repressing SPTAN1, Oncotarget 8 (35) (2017) 58098.